Article

Application of Terahertz Nondestructive Testing Technology in the Detection of Polyethylene Pipe Defects

Hailiang Nie,* Fengdan Hao, Litao Wang, Qiang Guo, Hongda Chen, Junjie Ren, Ke Wang, Wei Dang, Xiaobin Liang, and Weifeng Ma
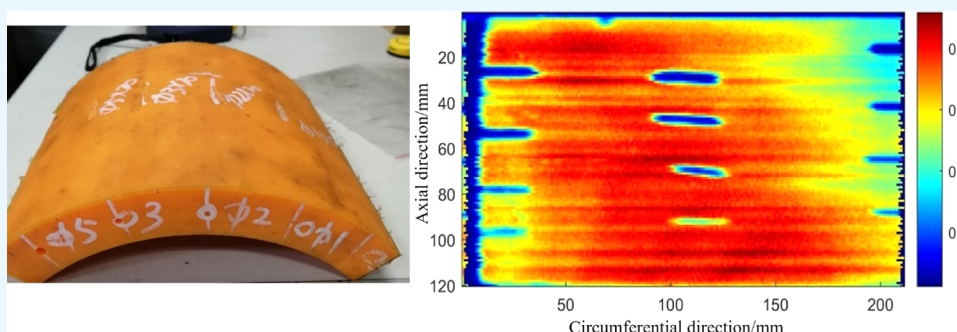
Read Online

| ACCESS | Metrics & More | Article Recommendations |

ABSTRACT: At present, polyethylene pipeline is widely used in urban gas projects, but a relatively mature and reliable nondestructive testing technology has not been formed. Therefore, it is urgent to develop a new nondestructive testing technology to meet the increasing demand for inspection of non-metallic pipes. The terahertz testing technology and related equipment have played an increasingly important role in the nondestructive testing of many nonmetallic structures, but they have not been applied to polyethylene (PE) pipes. In this work, terahertz time-domain spectroscopy was used to detect prefabricated defects inside the PE pipe specimens. The results show that the terahertz nondestructive testing technology can be used to detect common defects in nonblack PE pipes with a detection error of less than 10%. Higher-power terahertz devices can detect defects in black PE pipe, while lower-power terahertz devices cannot. Because the black PE pipe contains carbon and has a strong absorption of terahertz waves. The penetration of lower-power terahertz devices to the black PE pipe is not enough, resulting in a low resolution of the imaging. The results of this work may promote the progress of the nondestructive testing technology of nonmetallic pipelines.

1. INTRODUCTION

In recent years, the use of nonmetallic pipelines has increased in environmental protection projects, water supply projects, urban gas projects, etc. High-density PE pipes have gradually replaced traditional steel pipes and cast-iron pipes in medium- and low-pressure gas transportation because of their good corrosion resistance, absence of leakage, high strength and toughness, excellent flexibility, easy handling and installation, etc.; thus, they have become the preferred pipes for urban gas transportation.[1] The safety of nonmetallic pipelines has also attracted increasing attention, and its evaluation will attract large economic interests and will undergo future development.[2] 163 cases of PE pipeline failure in 4 companies were investigated, and it was found that the third-party damage accounted for 59% of the cases. Third-party damage refers to the man-made damage to the oil and gas pipeline, except the owner, construction company, and operation and management company. Third-party damage generally results in the loss of pipeline material. In recent years, the research field on damage detection in nonmetallic pipe structures has rapidly developed,

mainly focusing on straight pipes and pipe joints for nonmetallic pipes.[3] At Dalhousie University (Canada), piezo-electric ceramics were used to study the damage at the joint of nonmetallic pipes.[4] The torsional-mode-guided wave probe designed by Ecole Centrale de Lyon (France) was used to study the guided wave response and damage characteristics of nonmetallic pipelines.[5] At the University of Rome (Italy), simulations and experimental studies were carried out on the groove damage on nonmetallic circular rods via Gaussian-pulse-guided wave excitation.[6] Theoretical studies achieved good results, and satisfactory results were obtained in laboratory experiments. However, due to the lack of testing

equipment suitable for practical engineering, these methods can only be used in research laboratories and have not been used in practical engineering applications. In addition to the above conventional detection methods, some scholars have also developed unconventional detection methods, among which air-coupled ultrasonic detection technology has made great progress. Arno[7] has proved that it is possible to detect artificial defects using air-coupled ultrasonic inspection in thin polymer pipe walls; however, it is challenging to separate defects from normal variation in the measured signal.

Terahertz (THz) radiation refers to electromagnetic waves with frequencies ranging from 0.1 to 10 THz (1 THz = 10^{12} Hz), low energy (4.1 meV), a high signal-to-noise ratio, high resolution, and other characteristics, and is used in the field of nondestructive testing.[8] Since the 1990s, scientists have been working on devices that transmit and receive THz waves.[9] In 2008, Stoiks[10] applied THz time-domain spectroscopy (TDS) to nondestructive testing of aircraft fiberglass composites and evaluated the degree of thermal damage using simple amplitude two-dimensional images. Owing to its continuous development, the THz testing technology and related equipment will play an increasingly important role in the nondestructive testing of nonmetallic pipes.

Researchers have conducted extensive investigations in the field of THz nondestructive testing of nonmetallic materials and made some progress. Peters et al.[11] analyzed and calculated the THz time-domain spectrum of PE samples and obtained their stratified thickness without knowing the sample refractive index. Im et al.[12] studied the THz transmission of thick fiber-wound composites, analyzed the obtained time-domain spectrum in detail, and verified the feasibility of THz-TDS and imaging for nondestructive testing of composite materials. Wietzke et al.[13] carried out a number of studies in the field of nonmetallic nondestructive testing and used the THz continuous imaging system to detect internal defects in nonmetallic materials, such as PE. The results show that the THz imaging technology has good application prospects for detecting defects in nonmetallic materials, such as delamination, inclusion, mechanical damage, and thermal damage. Redo-Sanchez et al.[14] used a portable THz system to study materials such as gypsum artwork and carbon fibers and found that THz spectroscopy has an excellent spectral resolution for plastic samples; they obtained accurate information on the bonding condition and sample of binder in the sample.

Many research institutes have also studied the THz nondestructive testing technology for pipelines. Hong et al.[15] used the THz reflection imaging technology and the THz time-domain spectral transmission technology to detect PE electric fusion joints (inclusions, delamination, and other defects); they were able to clearly identify the inclusions (wire) and burial defects in the samples. Qiang[16] measured the thickness of a PE pipe via THz-TDS and carried out defect detection tests. His research mainly focused on theoretical and feasibility studies. Chen[17] proposed a sample feature recognition algorithm based on THz-TDS and proposed a feature recognition model. This model overcame the issues of spectral feature similarity recognition, feature defect recognition, and signal denoising in THz detection, laying a theoretical foundation for the THz detection technology.

From the abovementioned studies, it can be seen that THz nondestructive testing has developed rapidly in recent years, and a large number of research results have been obtained.

However, research institutions mainly focus on defect detection in flat materials and obtain good laboratory test results; however, in actual pipelines, the structure has a given curvature.

Whether the internal defects of such nonplanar structures can be detected and identified using the existing THz technology remains to be further verified. In this work, a method for the preparation of pipes with defects was mainly developed for PE pipes, which are widely used in urban gas transportation systems. Typical defects with a minimum size of 2 mm were prefabricated in PE pipes. Using the THz-TDS technology, the prefabricated defects were successfully detected. These results provide theoretical and technical support for the detection of defects in nonmetallic pipes.

2. MATERIALS AND SAMPLES

This study focuses on scratch damage defects on the surface of PE pipes as well as damage defects internal to the pipe material. Two types of pipeline materials were studied, namely yellow and black pipes.

The pipe samples used in this work are yellow and black PE pipes produced by Huida Pipe Industry with an outer diameter of 315 mm and a wall thickness of 30 mm. When manufacturing defects, 1/4 of the circumferential pipe section was considered, and different sizes and types of defects were fabricated at different locations on the pipe section using different drill bit sizes. Buried defects and inner surface defects were distributed at the two end faces of the pipe section. Outer surface defects were distributed in the middle axial direction of the pipe section, and the defects were elongated along the axial direction of the pipe section. A perpendicular drill was used to fabricate the buried and inner surface defects at the two end surfaces. When fabricating buried defects, the center of the drill bit was located in the middle of the wall; on the other hand, when fabricating inner surface defects, the center of the drill bit was at a depth of 1/2 of the diameter of the bit from the inner surface of the pipe segment. The diameter of the bit was used to control the diameter of the buried defects and the inner surface defects, and the depth of the drill was used to control the axial length of the defects. Outer surface defects were fabricated by drilling the bit perpendicular to the outer wall of the pipe segment. After drilling to the desired defect depth, the bit could move slowly along the axis of the pipe segment while cutting the material of the pipe body until the moving distance reached the desired defect length. The different defect types and sizes are listed in Table 1; the minimum defect diameter was 2 mm. The yellow and black PE tube samples are shown in Figure 1.

Table 1. Defect Types and Sizes

defect type	defect diameter (mm)	defect length (mm)
outer surface defect	2/3/4/5	25
buried defect	2/3/4/5	30
inner surface defect	2/3/4/5	15

The defects were fabricated directly on the nonmetallic pipe sections, and the samples were finally cut into tiles. This permitted not only to retain the curvature of the nonmetallic pipes themselves but also to reduce the space occupied by the samples, thereby easing their transportation, which lays a foundation for the indoor simulation of the field nondestructive testing of pipelines.
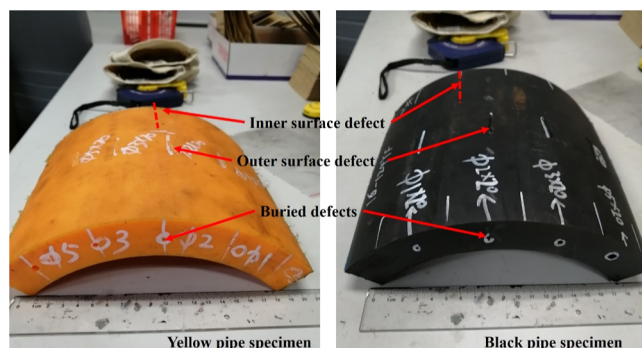
Figure 1. Photographs of the PE pipes with prefabricated defects.

3. TEST METHODS

3.1. Experimental Equipment. In this work, the T-Ray 5000 smart TCU control unit produced by API Corporation and a manipulator are used. The T-Ray 5000 intelligent TCU control unit contains a laser source and has many practical functions such as ultra-high-speed optical delay scanning to obtain THz waveforms, display of digital THz waveforms, numerical analysis, and transmission of test reports over the network. The laser source is made of mode-locked titanium sapphire, with a pulse width of 100 fs, an average output power of 20 mW, and a detection spectrum width of 0.2-2.5 THz. The sampling interval is 0.1 ps. The focusing lens diameter is 75 mm, and the spot diameter is about 2 mm with a Rayleigh length of 5−50 mm (the thickness of the test sample is 30 mm). The sample surface was scanned in steps of 1 mm during the detection process. The detection data was stored in a computer, and the defect image was obtained after processing using self-developed software. The THz detection device is shown in Figure 2.
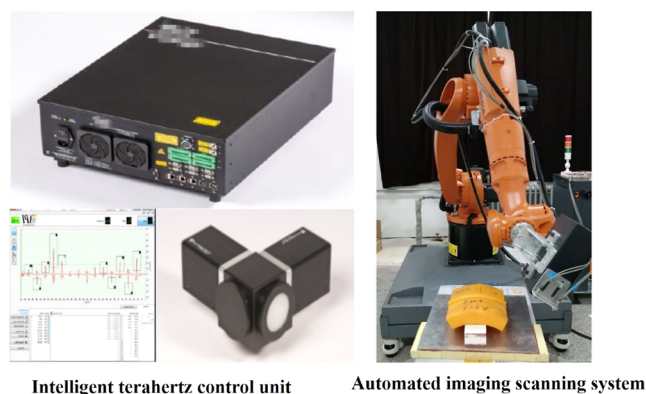

Figure 2. THz detection equipment.

During the experiments, we found that defects in black PE pipe could not be detected with the T-ray 5000, so we chose TK-LAB from Terakalis for alternative, equipped with optical devices with an average output power of 2 mW and a frequency range of 100−600 GHz. The focusing lens diameter is 60 mm, and the spot diameter is about 2 mm with a Rayleigh length of 3−40 mm. This device is only used in the detection of black PE pipe samples.

3.2. Principle of Defect Detection. The main purpose of this paper is to verify that the THz nondestructive testing technology can be applied to the defect detection of polyethylene (PE) pipeline engineering. The specific signal processing process is not the focus of this paper, so this paper adopts the data processing software of the test equipment to process the THz signal. Here, we only describe the basic principle of signal processing without describing the specific operation process in detail.

3.2.1. THz Imaging Technique. The THz imaging system was used to process and analyze the reflection spectrum information (including the amplitude and phase information) of the imaged sample, and the THz image of the sample was thus obtained. The THz imaging system is equipped with an image processing device and a scanning control device.

The THz time-domain spectral imaging system acquires three-dimensional (3D) space and time data [i.e., two space (x,y) axes and one time axis]. Using this 3D dataset, THz images of a series of samples can be obtained. In addition, because the THz image at a time point contains very little information (only the waveform information from one detection point), it is usually necessary to obtain the whole 3d dataset for defect reconstruction. The reconstruction of THz images is usually based on specific parameters of the THz time-domain waveform or the delay time of the peak position. At present, there exist mainly five methods for sample reconstruction:

(1) Time-of-flight imaging: the time delay information of each pixel is used to image the THz signal. This imaging method reflects the refractive index to THz radiation of the sample.

(2) Time-domain maximum value, minimum value, and peak value imaging: the maximum value, minimum value, or the difference between the maximum and minimum values of the THz time-domain signal in each pixel is used for imaging; the time-domain maximum-value imaging reflects the extinction coefficient of the sample to the THz wave.

(3) Specific-frequency amplitude (phase) imaging: the amplitude (phase) value of the THz frequency-domain signal at a certain frequency in each pixel is used for imaging.

(4) Power spectral imaging: the image information is obtained by integrating the square of the amplitude of the THz frequency-domain signal of each pixel within a certain frequency range.

(5) Pulse-width imaging: using the pulse-width imaging of the main peak of the THz radiation, the imaging model mainly reflects the dispersion characteristics of an object, and it can clearly present the outline of an object.

The detection of internal defects in structures can be carried out by analyzing the two-dimensional scanning image in the results.

In THz imaging, two-dimensional scanning imaging is performed on the row and column of a pixel in the detection area, where the horizontal axis indicates the position of the row or column and the vertical axis indicates the signal strength at the corresponding time of flight. Two-dimensional scanning imaging can be used to locate and analyze a defect, and the flight time corresponding to the defect can be used to analyze the depth direction of the defect. In addition, the defect characteristics in the THz time-domain waveform can be extracted, and the imaging analysis of the measured object can be carried out according to these characteristics.

3.2.2. Calculation Principle of the Defect Height. When THz waves propagate in different media, both transmission

and reflection occur at the interface, as shown in Figure 3. Assuming that the sample is isotropic and the THz wave is
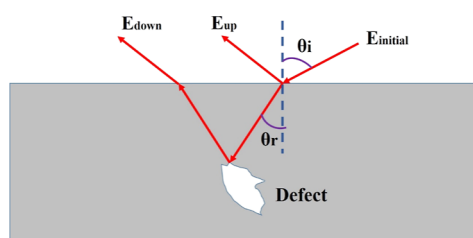

Figure 3. Reflection principle of THz waves.

incident at an angle θ_i, a THz echo E_{up} is generated at the air—medium interface due to the change in the refractive index. The transmitted THz wave is reflected on the upper surface of the defect. After the time difference ΔT, the detector detects the THz echo E_{down} successively.

There is a linear relationship between the buried depth of the defect and the flight time difference of the THz echo. The reflected single-point thickness extraction model is as follows

$$d = \frac{c\sqrt{n^2 - n_0^2 \sin^2 \theta_i}}{2n}(T_{up} - T_{down})$$
$$= \frac{c\sqrt{n^2 - n_0^2 \sin^2 \theta_i}}{2n}\Delta T \tag{1}$$

where n and n_0 are the refractive index of air and the material to be measured, respectively; T_{up} and T_{down} are the flight times of E_{up} and E_{down}; and c is the speed of light in air. When a THz wave is incident vertically, the single-point distance extraction model can be simplified as

$$d = \frac{c}{2}(T_{up} - T_{down}) = \frac{c}{2}\Delta T \tag{2}$$

According to the time difference between the two peaks, that is, the flight time difference, the characteristics of the flight time difference of THz waves in different materials can be obtained using the peak extraction technology, and the buried depth of the upper surface of the defect can then be calculated. The peak extraction technology is used to identify the defect characteristic waveform of the detection signal by comparing the actual detection signal with the standard test block detection signal, combined with the set threshold of frequency and amplitude. Using the same principle, the buried depth of the lower surface of the defect can be calculated. The height of the defect can be calculated by subtracting the buried depth of the lower surface of the defect from the buried depth of the upper surface of the defect.

4. RESULTS

4.1. THz Wave Refractive Index and Absorption of Materials. The refractive indices and absorption coefficients for the used materials of the THZ wave at different wavelengths were measured, as shown in Table 2. It can be seen that the THZ absorption coefficient of the black PE pipe is much higher than that of the yellow PE pipe. This is because the carbon black is added to the black PE pipe to prevent ultraviolet aging, and the carbon black absorbs a large amount of THZ wave.

4.2. Defect Detection in Yellow PE Pipe Samples.
4.2.1. Two-Dimensional Scanning Image of the Specimens.

Table 2. Refractive Index and Absorption Coefficient of Tested Materials to THz Wave

	refractive index		absorption value/m^{-1}	
wavelength/μm	yellow PE pipes	black PE pipes	yellow PE pipes	black PE pipes
70.5	1.554	1.561	81.52	99.54
96.5	1.549	1.551	53.79	74.79
118.8	1.546	1.548	51.63	71.63
122.4	1.542	1.546	48.87	68.87
158.5	1.536	1.542	42.78	62.78
184.3	1.53	1.538	23.80	43.80
214.6	1.523	1.528	22.96	42.96

The circular plane image of the prefabricated defect was obtained using the 2nd method (time-domain maximum value, minimum value, and peak value imaging), as shown in Figure 4, where the color depth represents the reflected wave
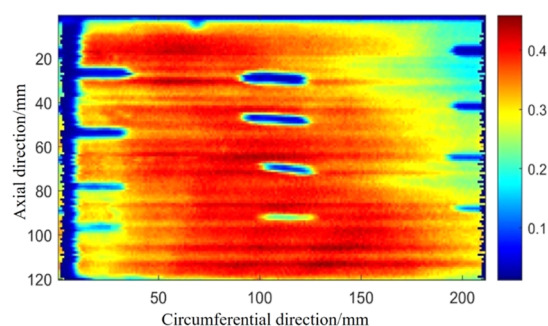

Figure 4. Toroidal two-dimensional scanning image of the defects.

amplitude normalized by the reflected wave/incident wave. As can be seen from the figure, there are four rows and three columns of detected defects, as expected. It can be seen that the first column represents buried defects, the second column represents outer surface defects, and the third column represents inner surface defects. The diameter of the defects decreases from the first row to the fourth row. The detected defects are ranked as follows: first row: 1-1#, 1-2#, 1-3#; second row: 2-1#, 2-2#, 2-3#; third row: 3-1#, 3-2#, 3-3#; fourth row: 4-1#, 4-2#, 4-3#.

4.2.2. Tomographic Images of the Defects in the Direction of the Wall Thickness. The location map of the defects in the direction of the thickness of the sample can be obtained using the tomographic imaging method, a technique to superimpose the reflected signals of different thicknesses on the same scan line to show the defect characteristics of different thickness layers. In fact, THz waves will generate reflection and transmission at the interface between solids and gases. In the experiment, we adopted the reflection imaging method, which is based on the amplitude characteristics of the reflected waves. Therefore, the image contour will be deeper in some parts. The depth of the imaging color has no practical significance, but the position features reflected by it are relatively accurate, which can help us identify and calculate the geometric features of the structure.

The tomographic images of the three defect positions in the first row were extracted, as shown in Figure 5. In the figure, the ordinate is the scanning time, and the abscissa is the axial scanning position. In the figure, the shallower contour on the uppermost layer is the result of the superposition of reflected waves on the upper surface of the sample, while the contour
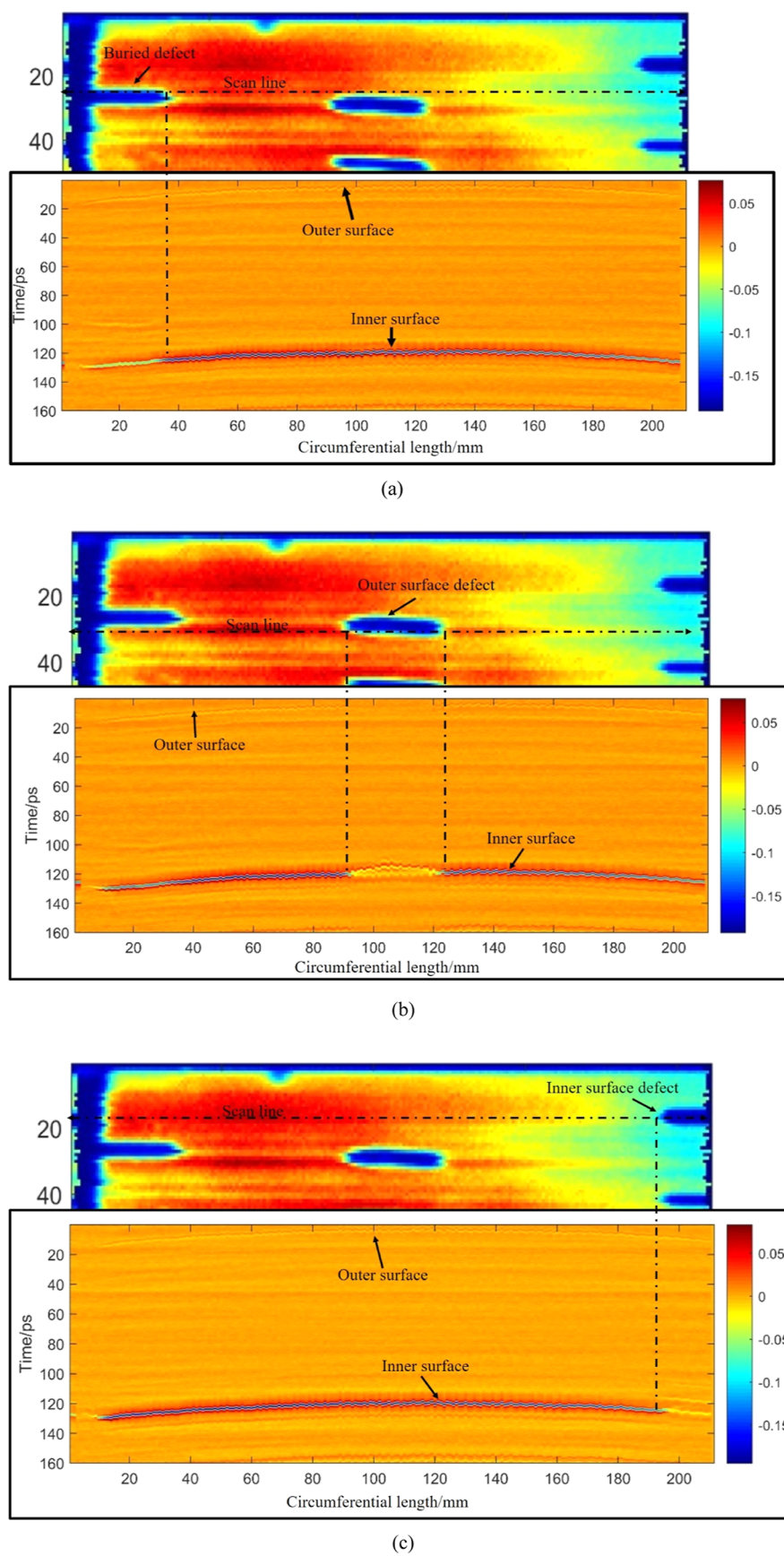
Figure 5. Tomographic image of the defects at the first row of Figure 4: (a) 1-1#, the buried defect on the left, (b) 1-2#, the external surface defect in the middle, (c) 1-3#, the inner surface defect on the right.

with the deepest color on the lower layer is the result of the superposition of reflected waves on the lower surface of the sample.

From Figure 5a, it can be seen that the buried defect gives rise to a steep contour, which is the result of the superposition of reflected waves on the upper surface. This contour is located between the upper and lower surface contours; the contour is not clear due to the diffuse reflection of waves on the lower surface of the defect.

Figure 5b shows the existence of defects on the upper surface, which leads to discontinuous fuzzy segments in the contour after the reflection waves on the upper and lower surfaces are superimposed. This is because the diffuse reflected waves on the lower surface of the THz wave on the outer surface defect cause the received reflected wave amplitude to become smaller, and the image is not clear. Therefore, the main characteristics of the outer surface defects are discontinuous fuzzy segments in the image profile of the reflected wave on the inner and outer surfaces.

Figure 5c shows the existence of an inner surface defect (the profile of the surface reflection wave is a discontinuous fuzzy segment). At the same time, on the surface and under the surface imaging profile between a profile, the outline of the inner surface defect of reflected wave imaging results; thus, imaging characteristics of inner surface defects, the surface profile of imaging discrete fuzzy segment. On the other hand, there is an imaging profile between the inner and outer surface profiles.

The distribution of defects in the thickness direction of the sample can also be analyzed by extracting the single waveform of the defects. The single waveform of three defects in the first row is shown in Figure 6. It can be seen that the amplitude of the reflected wave in the area without defects is larger, with the amplitude changing from positive to negative and back to positive; on the other hand, for the area containing defects, the amplitude of the reflected signal is smaller.

As can be seen from Figure 6a, the reflected signal of the buried defect presents two continuous peaks, one positive and one negative.

As can be seen from Figure 6b, the reflected signal from the outer surface defect presents multiple positive and negative interlaced continuous peaks.

As can be seen from Figure 6c, the reflected signal from the inner surface defect presents two discrete positive peaks.

4.2.3. Axial and Circumferential Dimensions of the Defects. The axial dimension (La) and the circumferential dimension (Lw) of a defect can be calculated from the experimental results (as shown in Figure 7). The calculation method is as follows: the axial and circumferential lengths of the defect are both 1 mm, so the pixel size is $1 \times 1 \text{ mm}^2$. La and Lw can be calculated by measuring the number of pixel points of defects in Figure 4. The measurement results are shown in Table 3. Compared with the actual defect size, the measurement error is about 10%.

4.2.4. Defect Height Calculation. The height of the defect is calculated as shown in Figure 8. The height of the defect can be calculated by determining the flight time of the upper and lower surfaces of the defect, as shown in Figure 9. Only buried defects can be used to calculate their height. Considering that the THz beam diameter is very small, only about 2 mm, and the sample thickness is not large, the beam dispersion can be ignored when calculating the defect size. The calculation
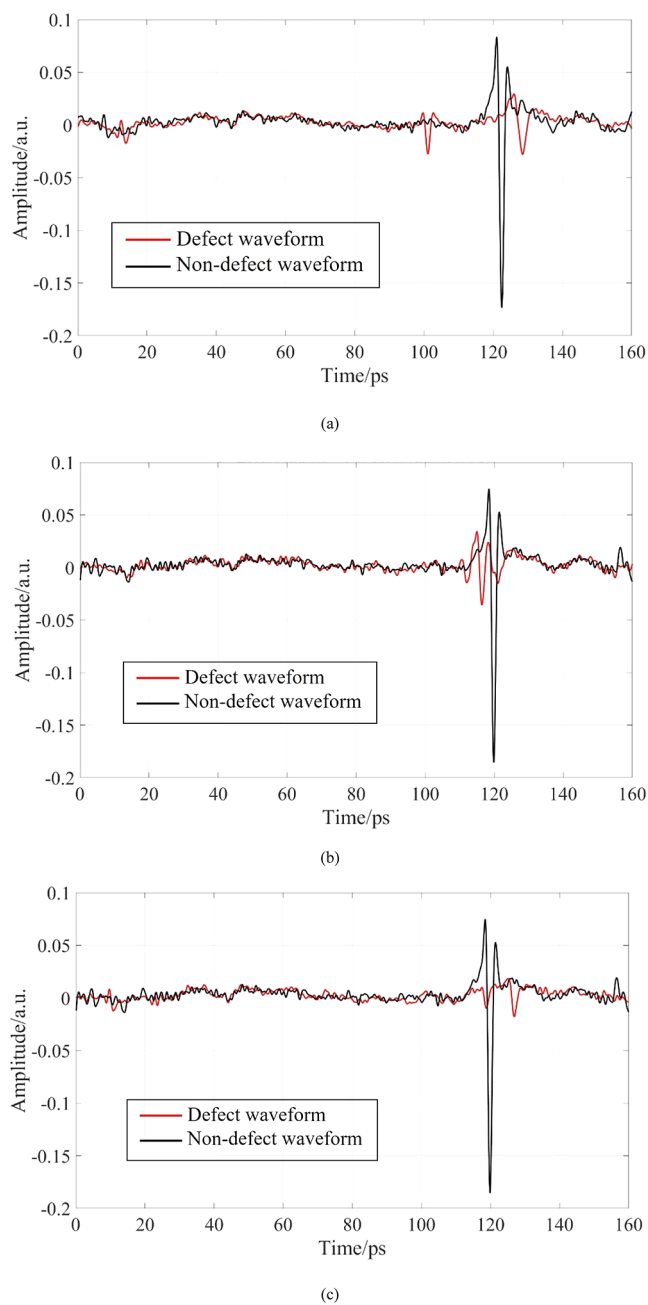

Figure 6. Comparison between the defect and non-defect waveforms at the first row: (a) 1-1#, (b) 1-2#, and (c) 1-3#.
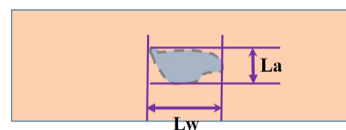

Figure 7. Schematic of the axial and circumferential dimensions of a defect.

results are shown in Table 4, and the calculation error is less than 10%.

4.3. Defect Detection in Black PE Pipe Samples. T-ray 5000 series equipment was also used to detect the sample of black PE pipe. The two-dimensional imaging results of the black PE pipe sample are shown in Figure 10. It can be seen from that when T-Ray 5000 series equipment is used to detect

Table 3. Calculated Defect Dimensions

ID	La (mm)	Lw (mm)	ID	La (mm)	Lw (mm)	ID	La (mm)	Lw (mm)
`	5	28	1-2#	5	31	1-3#	6	16
2-1#	5	27	2-2#	4	31	2-3#	4	16
3-1#	3	27	3-2#	3	29	3-3#	3	16
4-1#	2	29	4-2#	2	28	4-3#	2	16

Table 4. Calculated Defect Heights

ID	H (mm)	error (%)
1-2#	4.8	4
2-2#	3.9	2.5
3-2#	2.9	3.3
4-2#	1.8	10
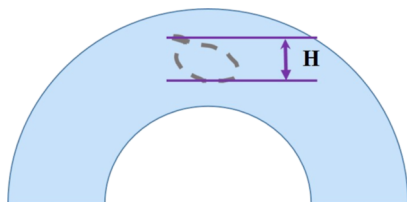
Figure 8. Diagram of the height of a defect.
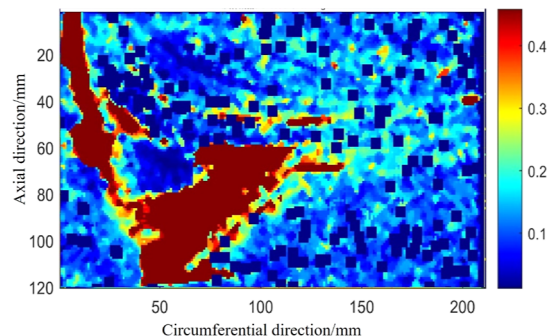
Figure 10. Two-dimensional imaging results for the black PE pipe sample.

the black pipe, the THz waveform cannot detect the defect signal. After analysis, it is found that the T-Ray 5000 equipment we used is a time-domain spectral system with low energy (the power is 550 W), while the black PE tube contains carbon and has strong absorption of THz waves. The penetration of T-Ray 5000 to the black PE tube is not enough, resulting in a low resolution of the imaging.

To verify the above analysis, we selected a higher-power THz detection device Terakalis TK-Lab (the power is 4.4 kW) to test the same black PE tube sample. The disadvantage of this device is that the original detection platform only contains a translational carrier platform, which cannot realize equidistance vertical scanning of test sample surfaces. The imaging results of black PE pipe with Terakalis TK-Lab series equipment are shown in Figure 11. It can be seen that the defect signal can be detected by Terakalis TK-Lab. The reason is that the equipment has higher power and has a stronger penetration ability to carbon.

Through the above analysis, it can be seen that there are problems in the black tube defect detection as follows:

(1) Higher-power THz devices can detect defects in black PE pipe, while lower-power THz devices cannot.
(2) In reflection mode, the detection effect is not ideal, and this is the large curvature artifacts existing equipment platform (Terakalis TK-Lab) can only along the planar scanning contradiction has much to do, without a
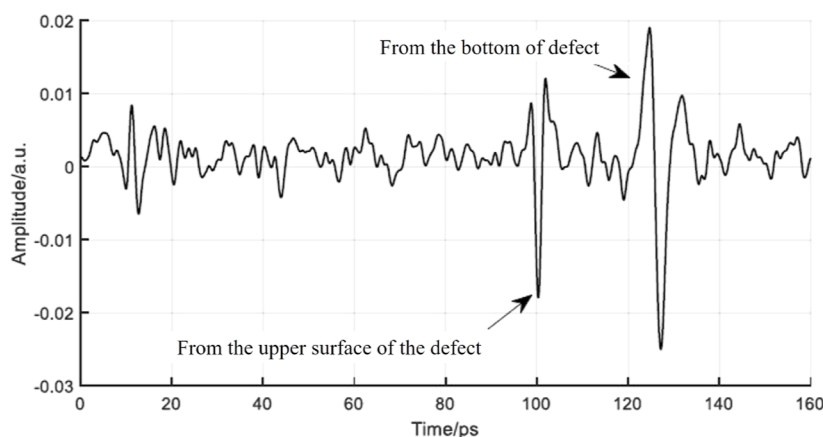
change in the angle probe and test face case, most of the reflected signal cannot be received, if the proper scanning mechanism (e.g., mechanical arm), the effect will be greatly improved.
(3) In addition to the defects, you can also see from the picture of other different distribution of light and shade, these phenomena still because there is a radian workpiece tested, there is no guarantee that the position is always in the same plane, for testing prototypes (plane scan), detection results can reflect the change of position, which can be used in the actual detection of mechanical arm programing scan way, the problem can be solved by keeping the distance between the probe and the workpiece always consistent.
(4) If the power increases, T-ray 5000 series equipment can also detect defects in black PE pipe.

5. DISCUSSION

5.1. Material Requirements. THz radiation penetrates into nonmetallic pipes but is completely reflected by metallic materials; thus, the THz detection technology cannot be used for metallic materials. In addition, carbon black strongly
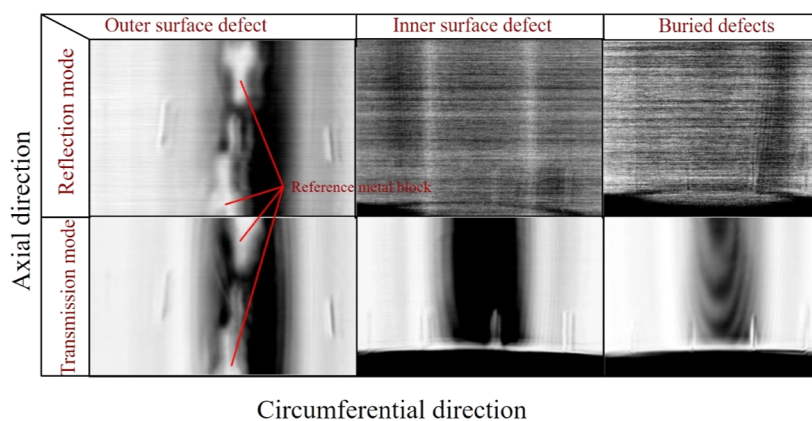

Figure 9. Defect height calculation using the flight time.

Figure 11. Imaging results of black PE pipe by Terakalis TK-Lab series equipment in France.

Table 5. Comparison of the THz Technology with Conventional Detection Techniques

NDT technology	characteristics
ultrasonic detection	low efficiency, unable to penetrate multilayer structures, and high loss in nonmetallic materials. The technology is mature
acoustic emission detection	the item under test must be loaded. One can only detect defects that are being generated and expanded. The technology is mature
thermal imaging	sensitive only to superficial defects. Immature technology
ray detection	as quarantine area is required for this test. The technology is mature
air-coupled ultrasonic detection technology	non-contact detection, the surface requirements are low, but the signal extraction and processing are more difficult
THz detection	good penetration depth, low energy, transient, and high resolution. This technique is noncontact; it can detect defects qualitatively and quantitatively and is capable of 3D imaging of defects

absorbs THz radiation, and black PE pipes often contain carbon black; thus, the THz technology cannot be used to detect defects in black PE pipes.

5.2. Structure Requirements. The THz detection technology is a noncontact detection method that requires radiation to be perpendicularly incident onto the workpiece surface. When there is a bulge or depression with a large curvature on the workpiece surface, the reflected wave may deviate from the path of the incident wave at a certain angle, resulting in the probe not being able to receive the reflected wave signal.

The time window of the existing THz data acquisition system is small, generally 160 or 320 ps, and the wave reflected beyond this window will not be collected. Therefore, the distance between the probe and the workpiece surface should be kept constant during the detection process to ensure that the waves reflected from the upper and lower surfaces can be received. Therefore, the THz detection technology requires a workpiece with a smooth surface and uniform thickness. A great variation in the thickness may lead to signal loss from the thicker parts.

5.3. Requirements for PE Pipe Equipment. THz detection of defects in PE pipes is feasible, but specific equipment requirements must be satisfied. A multidimensional transformation of the manipulator is necessary to obtain the 3D structural information of the sample to be tested. The manipulator can be guided to drive the probe for detection through system modeling.

5.4. Advantages and Disadvantages of THz Detection of Defects in PE Pipes. A comparison of the THz technology with other NDT technologies is provided in Table 5. The THz technology has the following technical advantages for defect detection in nonmetallic pipes: good penetration depth, low energy, transient, and high resolution. Furthermore, it is a noncontact technique, permits good positioning to be

achieved, provides qualitative and quantitative detection of defects, and is capable of 3D imaging of defects.

The THz detection technology also has certain limitations. The THz detection process must be perpendicular to the workpiece surface, which requires higher testing tooling, and a structure with a too large surface curvature cannot be tested with this technique. Additionally, it requires that the distance between the probe and the workpiece surface remain constant during detection to avoid data acquisition failure. Finally, the existing THz testing equipment is only suitable for indoor testing. Equipment and tooling for field testing have not been developed yet, and further research and development are needed.

6. CONCLUSIONS AND PROSPECTS

In this study, defects with a minimum size of 2 mm were prefabricated in typical PE pipe bodies. Using THz-TDS, the prefabricated defects inside the yellow PE pipe were successfully detected. At the same time, the circumferential and axial dimensions of the defects, as well as the height of the buried defects, were calculated. The results show that the THz nondestructive testing technology can be used to detect common defects in yellow PE pipes, and the detection error is less than 10%.

Higher-power THz devices can detect defects in black PE pipe, while lower-power THz devices cannot. Because the black PE tube contains carbon and has strong absorption of THz waves. The penetration of lower-power THz devices to the black PE pipe is not enough, resulting in a low resolution of the imaging.

The present study was conducted to verify the feasibility of indoor destructive testing. With further development in the THz detection technology, it is believed that it will be possible to use this technique in field detection. Real-time adjustment of the THz probe can be realized through real-time 3D optical

scanning of the surface of the pipeline; this method not only exhibits high detection efficiency but also greatly improves the detection accuracy. In addition, as this technique can be used to obtain 3D information, reconstructing the 3D shape of defects will become a research focus in the future. We have conducted some preliminary research work in this field and believe that 3D reconstruction of defects can be realized in the near future.

■ AUTHOR INFORMATION

Corresponding Author

Hailiang Nie — *Institute of Safety Assessment and Integrity, State Key Laboratory for Performance and Structure Safety of Petroleum Tubular Goods and Equipment Materials, Tubular Goods Research Center of CNPC, Xi'an 710077, China;* ⊙ orcid.org/0000-0001-5152-7978; Email: niehailiang88@163.com

Authors

Fengdan Hao — *China Promotion Association for Special Equipment Safety and Energy-Saving, Beijing 100029, China*

Litao Wang — *The Third Oil Transportation Department of Changqing Oilfield Branch of China National Petroleum Corporation, Ningxia 750006, China*

Qiang Guo — *Shaanxi City Gas Industry Development Co., LTD., Xi'an 710000, China*

Hongda Chen — *Institute of Safety Assessment and Integrity, State Key Laboratory for Performance and Structure Safety of Petroleum Tubular Goods and Equipment Materials, Tubular Goods Research Center of CNPC, Xi'an 710077, China*

Junjie Ren — *Institute of Safety Assessment and Integrity, State Key Laboratory for Performance and Structure Safety of Petroleum Tubular Goods and Equipment Materials, Tubular Goods Research Center of CNPC, Xi'an 710077, China*

Ke Wang — *Institute of Safety Assessment and Integrity, State Key Laboratory for Performance and Structure Safety of Petroleum Tubular Goods and Equipment Materials, Tubular Goods Research Center of CNPC, Xi'an 710077, China*

Wei Dang — *Institute of Safety Assessment and Integrity, State Key Laboratory for Performance and Structure Safety of Petroleum Tubular Goods and Equipment Materials, Tubular Goods Research Center of CNPC, Xi'an 710077, China*

Xiaobin Liang — *Institute of Safety Assessment and Integrity, State Key Laboratory for Performance and Structure Safety of Petroleum Tubular Goods and Equipment Materials, Tubular Goods Research Center of CNPC, Xi'an 710077, China*

Weifeng Ma — *Institute of Safety Assessment and Integrity, State Key Laboratory for Performance and Structure Safety of Petroleum Tubular Goods and Equipment Materials, Tubular Goods Research Center of CNPC, Xi'an 710077, China*

Complete contact information is available at:
https://pubs.acs.org/10.1021/acsomega.3c02701

Notes

The authors declare no competing financial interest.
The datasets generated and/or analyzed during the current study are not publicly available due to the company confidentiality requirements but are available from the corresponding author on reasonable request.

■ REFERENCES

(1) Schrock, J. Underground Plastic Pipe. *International Conference on Underground Plastic Pipe*; American Society of Civil Engineers: New York Ny, 2015.

(2) Stepanova, L. N.; Kabanov, s I.; Ramazanov, I. S.; Lebedev, E. Y.; Kireenko, V. V.; Vonsovskii, A. V.; Kinzhagulov, I. Y. Acoustic-emission testing of multiple-pass welding defects of large-size constructions. *Russ. J. Nondestr. Test.* **2015**, *51*, 540−545.

(3) Nara, T.; Takanashi, Y.; Mizuide, M. A sensor measuring the Fourier coefficients of the magnetic flux density for pipe crack detection using the magnetic flux leakage method. *J. Appl. Phys.* **2011**, *109*, 07E305.

(4) Cheraghi, N.; Riley, M. J.; Taheri, F. A novel approach for detection of damage in adhesively bonded joints in plastic pipes based on vibration method using piezoelectric sensors. In *IEEE International Conference on Systems, Man and Cybernetics 2005*; IEEE, 2005; Vol. 4, pp 3472−3478.

(5) Bareille, O.; Kharrat, M.; Zhou, W.; Ichchou, M. Distributed piezoelectric guided-T-wave generator, design and analysis. *Mechatronics* **2012**, *22*, 544−551.

(6) Pau, A.; Vestroni, F. Damage characterization in bars using guided waves. In *Proceedings of the XIX AIMETA Congress*: Ancona, 2009; pp 65−75.

(7) Römmeler, A.; Furrer, R.; Sennhauser, U.; Lübke, B.; Wermelinger, J.; de Agostini, A.; Dual, J.; Zolliker, P.; Neuenschwander, J. Air coupled ultrasonic defect detection in polymer pipes. *NDT&E Int.* **2019**, *102*, 244−253.

(8) Stoik, C. D.; Bohn, M. J.; Blackshire, J. L. Nondestructive evaluation of aircraft composites using transmissive terahertz time domain spectroscopy. *Opt. Express* **2008**, *16*, 17039−17051.

(9) Benicewicz, P. K.; Roberts, J. P.; Taylor, A. J. Scaling of terahertz radiation from large-aperture biased photoconductors. *J. Opt. Soc. Am. B* **1994**, *11*, 2533−2546.

(10) Stoik, C.; Bohn, M.; Blackshire, J. Nondestructive evaluation of aircraft composites using reflective terahertz time domain spectroscopy. *NDT&E Int.* **2010**, *43*, 106−115.

(11) Peters, O.; Wietzke, S.; Jansen, C.; et al. Nondestructive detection of delaminations in plastic weld joints. *35th International Conference on Infrared, Millimeter, and Terahertz Waves*; IEEE. 2010, 978-14244-6657-3/10.

(12) Im, K.-H.; Hsu, D. K.; Chiou, C. P.; et al. Influence of Terahertz Waves on the Penetration in Thick FRP Composite Materials. In *AIP Publishing Proceedings*; AIP Publishing LLC, 2014; pp 1568−1575.

(13) Jansen, C.; Wietzke, S.; Peters, O.; Scheller, M.; Vieweg, N.; Salhi, M.; Krumbholz, N.; Jördens, C.; Hochrein, T.; Koch, M. Terahertz imaging: applications and perspectives. *Appl. Opt.* **2010**, *49*, E48−E57.

(14) Redo-Sanchez, A.; Norman, L.; Brian, S.; et al. Non-destructive Imaging with Compact and Portable Terahertz Systems. In *AIP Publishing Proceedings*; AIP Publishing LLC, 2014; pp 1583−1586.

(15) Hong, W.; Liao, X.; Liu, Y. Nondestructive Evaluation of Electrofusion Joint of Polyethylene Pipeline Using Terahertz Wave. In *China Special Equipment Safety*, 2016. (in Chinese).

(16) Qiang, J.; Lingwie, Y.; He, Y. Deconvolution Algorithm of THz-TDS Polyethylene Thickness Measurement Based on Modified Autocorrelation Algorithm. *Infrared Technol.* **2020**, *42*, 473−482.

(17) Chen, S.; Han, X.; Lijuan, L.; et al. Research on Plastic Detection Based on Terahertz Time Domain Spectroscopy. *J. Changchun Univ. Sci. Technol.* **2017**, *05*, 17−20. (in Chinese).